Engineering Science and Technology, an International Journal 58 (2024) 101850

Contents lists available at ScienceDirect

Engineering Science and Technology, an International Journal

journal homepage: www.elsevier.com/locate/jestch

Full Length Article

A new RMF stirrer design to reduce mixing time

S. Bicakci [a], H. Citak [b], H. Gunes [c], M. Coramik [d], Y. Ege [d,*]

[a] Balikesir University, Faculty of Engineering, Department of Electric and Electronics Engineering, 10145 Balikesir, Turkey
[b] Balikesir University, Balikesir Vocational High School, 10145 Balikesir, Turkey
[c] Balikesir University, Faculty of Engineering, Department of Computer Engineering, 10145 Balikesir, Turkey
[d] Balikesir University, Necatibey Faculty of Education, Department of Physics, 10100 Balikesir, Turkey

ARTICLE INFO

Keywords:
ANSYS Maxwell
RMF Stirrer
FPGA
Adaptive Control Method
PWM Modulation
Mixing Time

ABSTRACT

The goal of this study is to develop an FPGA-based new rotating magnetic field (RMF) stirrer system that would reduce mixing time. To achieve this goal, it has been suggested that, unlike the literature, the mixing process is performed not only by a single magnetic fish rotating at the center but also by multiple magnetic fish rotating at symmetric positions. As the first step within such scope, ANSYS Maxwell® simulation software was used to design a stirrer core capable of realizing said proposition. The design was subsequently manufactured, and RST coils were wound. Being completed by the manufacturing of the electronic circuit to drive the coils, RST phases of the stirrer system were fed by PWM voltage with a phase difference of 120°. The myRIO® embedded system made use of the FPGA structure to control phases sequentially, generate PWM signals, and define the increment range for phase frequency. The ARM microprocessor structure of the myRIO® embedded system was utilized in the system for Adaptive control method. Programming of the myRIO® embedded system was achieved through the developed graphic-based LabVIEW® software. When the system was driven at 100% duty cycle, the magnetic force provided by the stator caused four magnetic fish with a 90° angle to each other to act as rotors, with two of the reciprocal magnetic fish rotating clockwise while the other two rotating counterclockwise. This enabled the mixing process to be more homogeneous and to be completed in a shorter period of time. Findings suggest that mixing time for water has been reduced by 35% in average. Experimental results on the structure, control and effects on reduction of mixing time of the RMF stirrer system developed within the scope of the study has been discussed in detail.

1. Introduction

Magnetic stirrers are predominantly used in chemistry, microbiology, biomedical and pharmaceutics laboratories, research and quality control laboratories in the food, paint and textile industries and, currently in particular, in the initial preparation phases of nanotechnology applications. Magnetic stirring is required in order to be able to stir liquids inside air-tight containers [1]. Electromagnetic stirring process can be induced in 3 different ways: horizontal, vertical and horizontal + vertical. Horizontal stirring is induced by a rotating magnetic field (RMF), while vertical stirring is induced by a traveling magnetic field (TMF) [2]. Magneto hydrodynamic (MHD) stirring occurs when both types of magnetic fields are applied simultaneously [3–5]. RMF Stirrers are actually axial flux synchronous motors [6–9]. The difference between synchronous motors and RMF stirrers is that the rotor is inside the stator. While the rotating magnetic field occurs inside the stator in a synchronous motor, it occurs on the upper surface of the stator core in the RMF stirrer. Such stirrers feature a magnetic fish (a short bar magnet with low pole strength) or the metallic liquid itself as the rotor [10]. No physical connection exists between the rotor and the magnetic field source, and the rotor follows the rotating magnetic field. The use of Rotating Magnetic Field Electromagnetic Stirring Systems (RMF-EMS) is widespread in the production process of continuously cast billets and blooms [11,12]. Another option to rotary stirring is axial stirring, also known as ''up and down'' stirring, which induces liquid movement parallel to the axis of the cavity. This type of flow is induced by a traveling magnetic field (TMF), which is generated by a linear motor. The utilization of RMF and TMF fields in MHD stirrers is widespread for conducting experimental investigations into the impact of liquid phase motion on heat and mass transfer during the crystal growth and solidification of metal alloys. MHD stirrers not only ensure toroidal flow in the solution with RMF, but also poloidal flow utilizing TMF

* Corresponding author.
E-mail address: yavuzege@gmail.com (Y. Ege).

https://doi.org/10.1016/j.jestch.2024.101850
Received 9 September 2023; Received in revised form 15 August 2024; Accepted 25 September 2024
Available online 9 October 2024

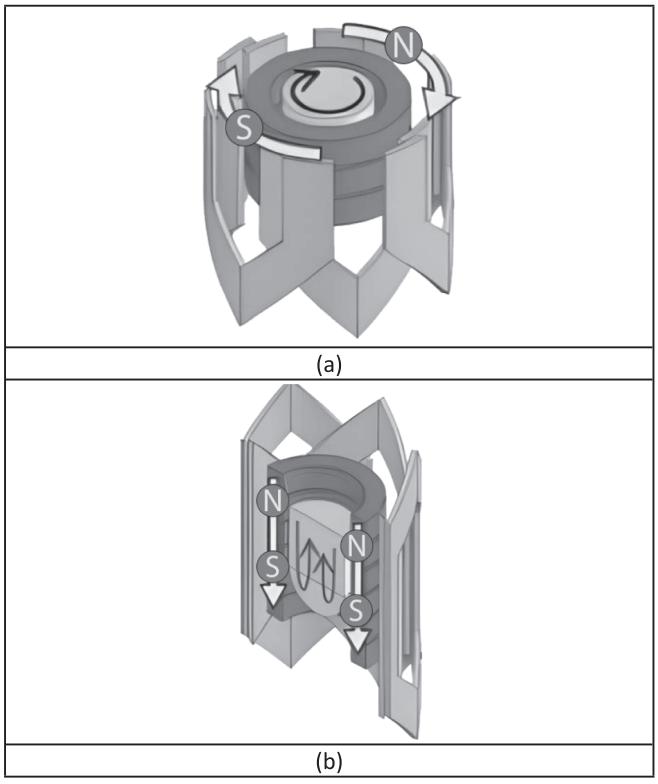

Fig. 1. Magneto hydrodynamic stirrer (MHD) a) RMF Stirrer, c) TMF Stirrer [15].

(Fig. 1). Therefore, MHD stirrers incorporate two independent coil systems [13–15].

2. Introduction

Magnetic stirrers are predominantly used in chemistry, microbiology, biomedical and pharmaceutics laboratories, research and quality control laboratories in the food, paint and textile industries and, currently in particular, in the initial preparation phases of nanotechnology applications. Magnetic stirring is required in order to be able to stir liquids inside air-tight containers [1]. Electromagnetic stirring process can be induced in 3 different ways: horizontal, vertical and horizontal + vertical. Horizontal stirring is induced by a rotating magnetic field (RMF), while vertical stirring is induced by a traveling magnetic field (TMF) [2]. Magneto hydrodynamic (MHD) stirring occurs when both types of magnetic fields are applied simultaneously [3–5]. RMF Stirrers are actually axial flux synchronous motors [6–9]. The difference between synchronous motors and RMF stirrers is that the rotor is inside the stator. While the rotating magnetic field occurs inside the stator in a synchronous motor, it occurs on the upper surface of the stator core in the RMF stirrer. Such stirrers feature a magnetic fish (a short bar magnet with low pole strength) or the metallic liquid itself as the rotor [10]. No physical connection exists between the rotor and the magnetic field source, and the rotor follows the rotating magnetic field. The use of Rotating Magnetic Field Electromagnetic Stirring Systems (RMF-EMS) is widespread in the production process of continuously cast billets and blooms [11,12]. Another option to rotary stirring is axial stirring, also known as ''up and down'' stirring, which induces liquid movement parallel to the axis of the cavity. This type of flow is induced by a traveling magnetic field (TMF), which is generated by a linear motor. The utilization of RMF and TMF fields in MHD stirrers is widespread for conducting experimental investigations into the impact of liquid phase motion on heat and mass transfer during the crystal growth and solidification of metal alloys. MHD stirrers not only ensure toroidal flow in the solution with RMF, but also poloidal flow utilizing TMF (Fig. 1). Therefore, MHD stirrers incorporate two independent coil systems [13–15].

The deposit which accumulates on the surface of the fluid due to the centrifugal force resulting from the rotating movement of the RMF is pushed downward by the TMF. The downward force generated by the TMF creates a downward flow near the wall. Said downward flow impacts the bottom surface and changes direction, creating an upward flow at the center which pushes up the lower part of the fluid level deformation. Consequently, fluid surface deformation is reduced. As RMF and TMF can be controlled independently, fluid level can be kept constant by adjusting the TMF current according to the deformation of the fluid level [16–18]. However, RMF-only stirrers are preferred for fluids with low electrical conductivity, such as aqueous solutions. In the literature, such stirrers are mostly utilized in fluid flow and crystal growth applications [19–22]. Furthermore, rotary stirring is employed in continuous casting or during the solidification of metallic melts, demonstrating its advantageous impact on the microstructure of the resulting ingots [23]. Two main effects may be observed: firstly, the RMF-driven convection promotes the transition from columnar to equi-axed dendritic growth; secondly, in many cases, a distinct grain refining is obtained. Nonetheless, it was also revealed that stirring a solidifying alloy might cause macro segregation [24,25]. RMF Stirrer was preferred in this study because of its aforementioned benefits and wide range of application. A new RMF Stirrer system has been developed in this study, which, unlike the literature, achieves mixing in a more homogeneous and shorter time frame. Said stirrer features four magnetic fish with a 90° angle to each other, where two of the reciprocal magnetic fish rotate clockwise while the other two rotate counterclockwise. Such rotation characteristic prevents deformation of the surface of the stirred liquid without the need of a TMF stirrer. This allows a mixture as would be in an MHD stirrer to be obtained within a shorter time. Experimental results on the structure, control and effects on reduction of mixing time of the RMF stirrer system developed within the scope of the study has been respectively explained in detail.

3. RMF stirrer core design with ANSYS Maxwell® simulation software

As the first step in the study, a core was designed, using ANSYS Maxwell® simulation software, for a new RMF Stirrer that would perform the stirring process both more homogeneously and within a shorter time by incorporating the rotation of multiple magnetic fish. The design process began by selecting a cylindrical disc with a diameter of 130 mm and height of 35 mm, adequate in size to hold below the necessary coils and above conventional 1 L beakers. AISI4140 mild steel was preferred due to its low H_c critical value. The 12-section core was created by opening 5 mm wide, 25 mm deep and 130 mm length canals which 150 winding coils made of 0.5 mm diameter copper wire will be placed on the upper surface of the cylindrical disc. During design trials, it was proposed that a steel ring made of the same material as the core should be placed at the center of the core in order to ensure that the rotating magnetic field created in the core by the PWM voltage applied to the RST coils with a phase difference of 120° would be able to rotate multiple magnetic fish. The inner diameter, outer diameter and height of such ring was made variable, thereby reducing the magnetic field magnitude at the core center to zero and enabling multiple magnetic fish located around the perimeter of the ring to rotate, as opposed to a single magnetic fish rotating at the center of the core. As a result of many trials regarding the dimensions of the ring, it was determined that the inner diameter of the steel ring should be 40 mm, its outer diameter 90 mm and its height 15 mm (Fig. 2a). Magnetic permeability and chemical components of the AISI4140 mild steel selected for the core and the ring are exhibited in Table 1. In addition, placement of the RST coils on the core during the magnetic analysis, as well as the current input directions for each phase is shown in Fig. 2.

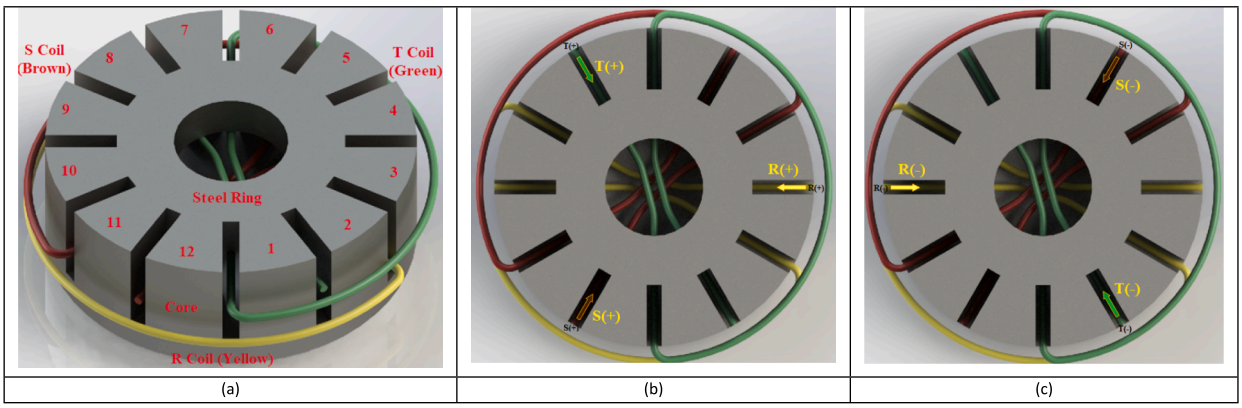

Fig. 2. (a) Core and RST coil designs for the Magnetic Stirrer, (b) Current inputs for the [R(+), S(+), T(+)] phases, (c) Current inputs for the [R(−), S(−), T(−)] phases.

Table 1
Chemical composition of the AISI4140 mild steel in terms of % weight and its magnetic permeability.

Material	C	Si	Mn	P	S	Cr	Mo	Ni	Magnetic Permeability (H/m)
AISI 4140	0.45	0.40	0.90	0.025	0.035	1.20	0.30	0.40	700–1000

During the analysis, currents were given to the RST (UVW) coils in [R(+), S(−), T(−)], [R(−), S(+), T(−)] and [R(−), S(−), T(+)] directions, respectively. These currents were provided by PWM voltage at 100 % duty cycle applied to the coils. In the study, PWM voltage was preferred with the idea that energy savings could be achieved by changing the duty cycle value. Fig. 3 shows the magnetic pole state, magnetic field magnitude and change determined on the core surface when currents of 1.5 A are applied to the RST coils in the [R(+), S(−), T(−)], [R(−), S(+), T(−)] and [R(−), S(−), T(+)] directions, respectively. As seen in Fig. 3, both a rotating magnetic field was created on the core surface and the magnetic field at the core center, which is the inner part of the steel ring, was reduced to zero. Subsequent to the aforementioned step, core channels were drawn for each phase, as well as a total of 12 "Polylines" along the center of the core sections, and magnetic field changes were determined along each polyline. Values at which the magnetic field is minimum, and maximum were determined along all polylines for each phase, and the locations on the core where a magnetic fish can rotate by phase changes were investigated. Using the ANSYS Maxwell® simulation program, magnetic field changes in the z direction were determined along polylines where only the magnetic fish could rotate. The change in magnetic field magnitude along 3 polylines for the R phase in the first position where the magnetic fish can rotate is shown in Fig. 4. The change in magnetic field magnitude along 3 polylines for the S phase and T phase at the first position where the magnetic fish can rotate is given in Appendix A. However, the change in magnetic field magnitude along 3 polylines for the R phase, S phase and T phase at the second position where the magnetic fish can rotate is given in Appendix B.

As seen in Fig. 4, Fig.A1 and Fig.B1, points at which the magnetic field is minimum and maximum along polylines for each phase are marked with markers m1, m2, m3 and m4, magnetic field magnitudes at said points were determined and noted on the core design. Then, for the first position, the rotation circle of the magnetic fish passing through the m3 and m4 points on Polyline 2, Polyline 3 and Polyline 4 was determined (Fig. 4). It was thereby understood that the magnetic fish which can be used during the experimental phase should not exceed the diameter of such circle (approximately 3 cm) (Fig. 4). It was therefore ensured that the length of the magnetic fish does not exceed 2 cm. Fig. 5 demonstrates which position a magnetic fish to be placed inside the circle will be under magnetic force in the RST phases, and that the direction of rotation will be clockwise. For each phase, the magnetic field magnitudes and direction changes at the positions of m3 and m4 markers on the core confirm that the magnetic fish will rotate clockwise. In addition, since the magnitude and direction change of the magnetic field at the m1 and m2 points on the polylines (Fig. 4) is the same for the first position, a second magnetic fish will be able to rotate in the same direction in the symmetry of the magnetic fish seen in Fig. 5.

The second circle position passing over the m3 and m4 markers where the magnetic fish can rotate on the core is seen in Fig. 6. When the magnetic field magnitude and direction changes at the m3 and m4 marker positions for each phase are examined in Fig. 6, it is understood in which position a magnetic fish placed within this circle bounded by the m3 and m4 markers will be in the RST phases and its direction of rotation will be counterclockwise. Furthermore, since the magnitude and direction of the magnetic field at points m1 and m2 on the polylines (Fig. B1) are the same for the first position, the second magnetic fish will be able to rotate in the same direction within the symmetry of the magnetic fish seen in Fig. 6. Thus, according to the ANSYS Maxwell® analysis results for the stirrer, it was confirmed that four magnetic fish could rotate at 90° angle between each other, with two of the reciprocal magnetic fish rotating clockwise and the other two rotating counterclockwise (Fig. 7).

4. Manufacturing of the RMF stirrer core according to the design and development of the electronics

In this phase of the study, American Iron and Steel Institute's AISI4140 mild steel was procured in a certain amount and been machined on the lathe into a cylindrical disc with a diameter of 130 mm and height of 35 mm. Then, in accordance with the design, in order to place the 150-winding RST (UVW) coils made of 0.5 mm diameter copper wire, 12-sections were created by opening 5 mm wide, 25 mm deep and 130 mm length canals on the upper surface of the cylindrical disc. While calculating the canal cross-section, the overlap of the RST (UVW) coils at the disc center and the ring height were taken into account. The sectioned disc was subsequently machined to have a diameter of 90 mm and depth of 15 mm from the center. Then, 150-winding RST (UVW) coils made of copper wire of 0.5 mm diameter were placed in the channels. Finally, a ring made of the same material, with an inner diameter of 40 mm, outer diameter of 90 mm and height of 15 mm, was placed in such section (Fig. 8a, b). The core was left under uniform magnetic field of magnitude 0.005 T for a day in order to remove the low stress resulting from the machining process and was rested for another

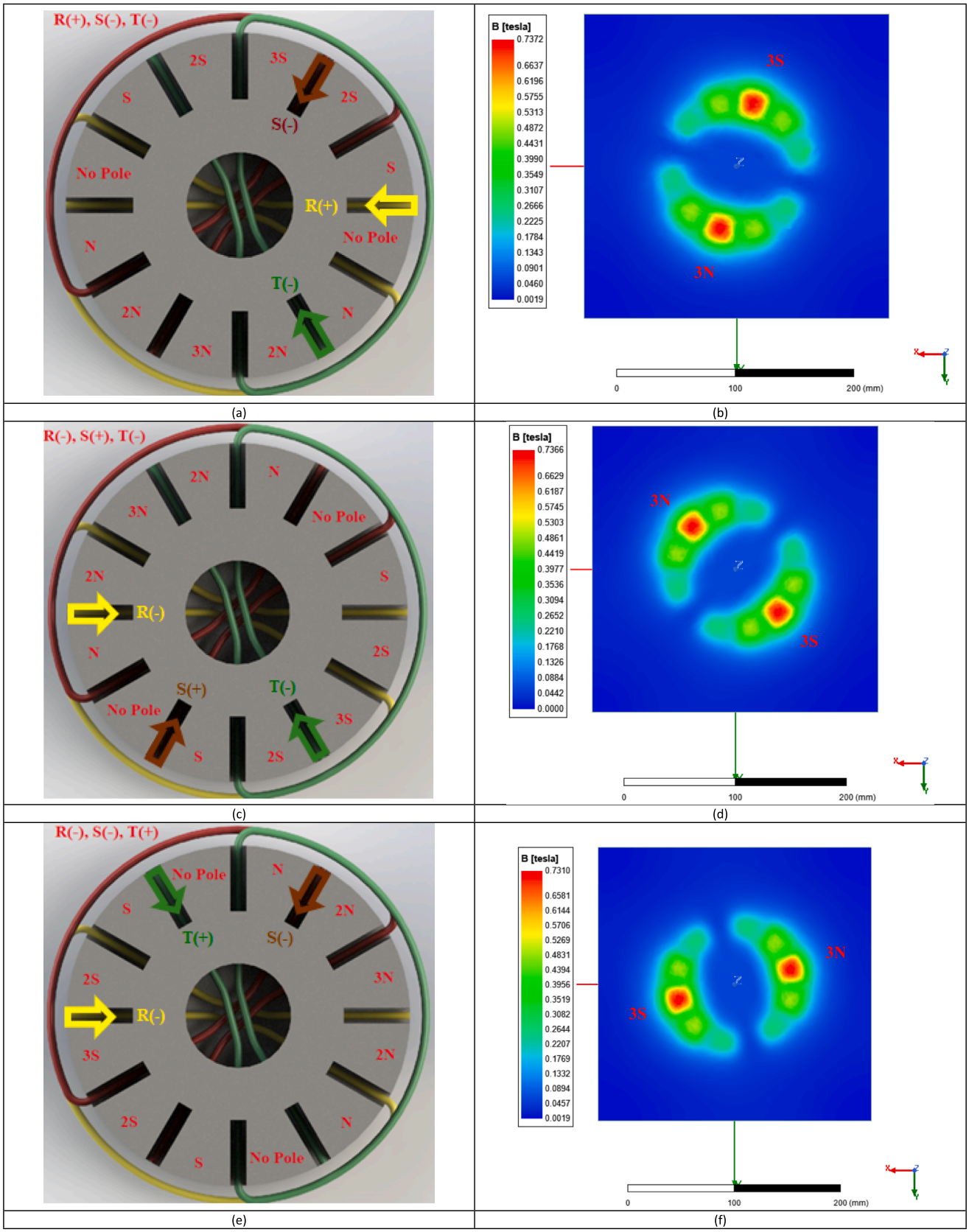

Fig. 3. Magnetic pole status and magnetic field distribution for the Magnetic Stirrer; (a, b) for phases [R(+), S(−), T(−)], (c, d) for phases [R(−), S(+), T(−)], (e, f) for phases [R(−), S(−), T(+)].

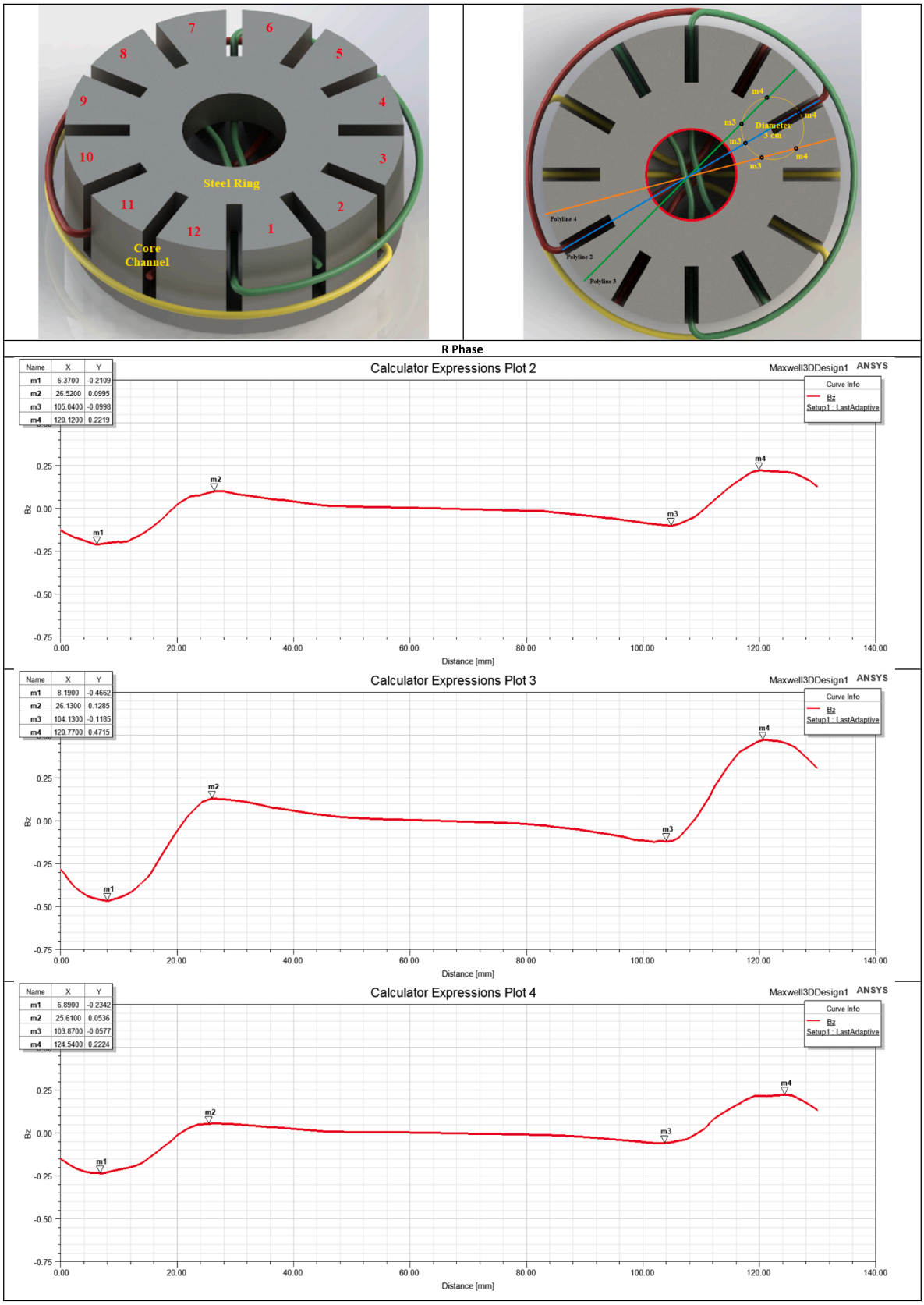

Fig. 4. Change in magnetic field magnitude along 3 polylines at the first position where the magnetic fish can rotate on the surface of the Magnetic Stirrer core (for R Phase).

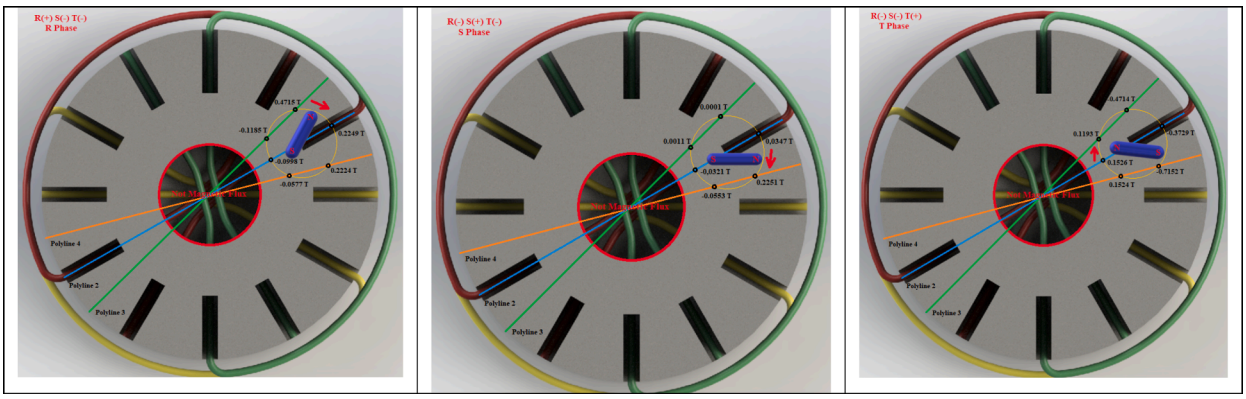

Fig. 5. The position, at each phase, of a magnetic fish which could rotate clockwise on the stirrer core.

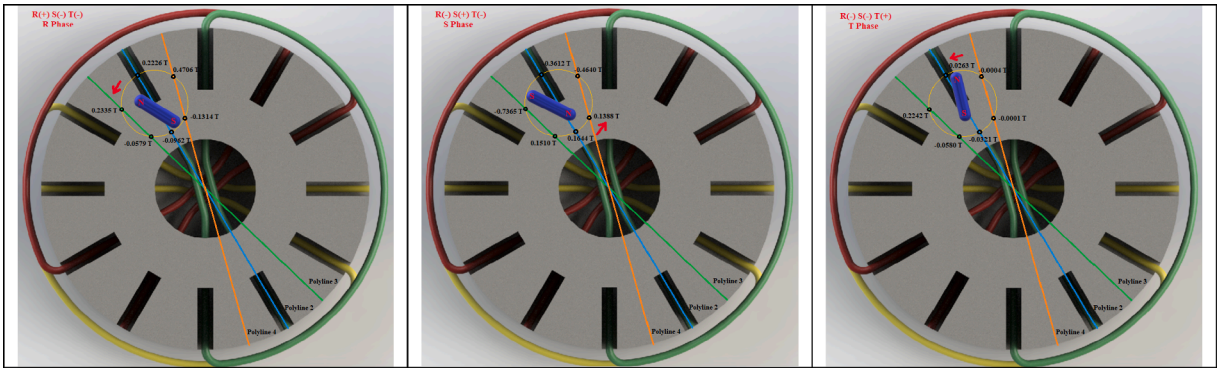

Fig. 6. The position, at each phase, of a magnetic fish which could rotate counterclockwise on the stirrer core.

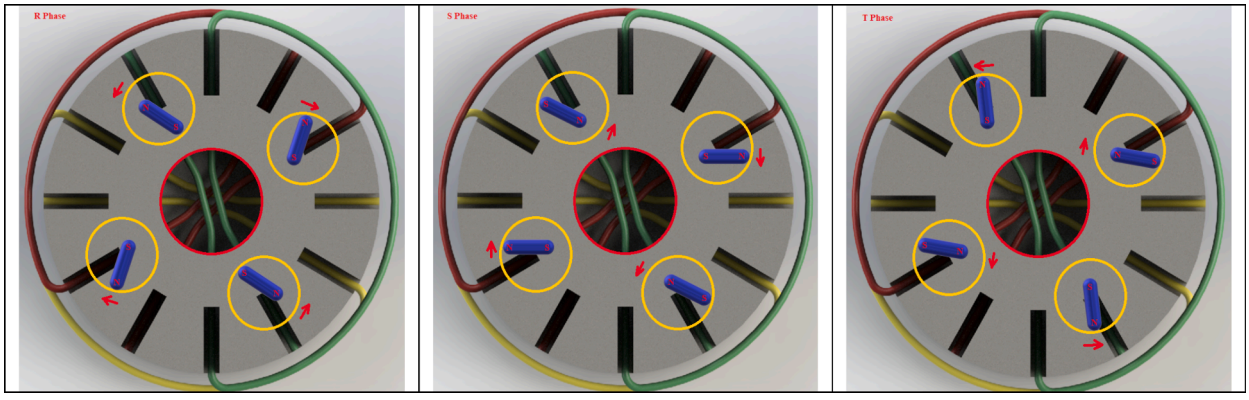

Fig. 7. The position, at each phase, of the four magnetic fish which could rotate on the stirrer core.

three days until the permanent magnetism disappeared. This time was determined by taking into account tesla meter measurements.

Manufacturing of the RMF Stirrer stator (core) was followed by the designing of the electronic driver circuit capable of applying 16 V PWM voltage to the coils for the R, S and T phases with a phase difference of 120 degrees (Fig. 3a). The coils were fed using an L298N step motor driver IC. This allowed application of currents of up to 3A to the coils. However, in the study, a constant current of 1.5 A was applied to the coils to prevent heating. This magnitude of current applied sequentially to the windings of the RST (UVW) phases according to the phase frequency did not cause heating. The FPGA structure within the NI myRIO® 1950 embedded system (National Instruments Corporation, Austin, TX ABD) was utilized in the study for sequential control of the phases, generation of the PWM signal and determination of the increment range of the phase frequency. The ARM microprocessor structure of the myRIO® embedded system was utilized in the RMF stirrer system to adjust the duty cycle value of the RMF voltage by Manual Control. However, in this study, the duty cycle value was selected as 100 %. LabVIEW® software interface was used to program the myRIO® embedded system. Block diagram and photograph of the RMF stirrer system developed within the scope of the study is demonstrated in Fig. 9a and Fig. 9b, respectively.

5. Developed LabVIEW software for RMF stirrer system

The programming of the myRIO® 1950 embedded system for the control of the RMF stirrer was done with LabVIEW® software (National Instruments Corporation, Austin, TX ABD). The 3 coils in the RMF stirrer

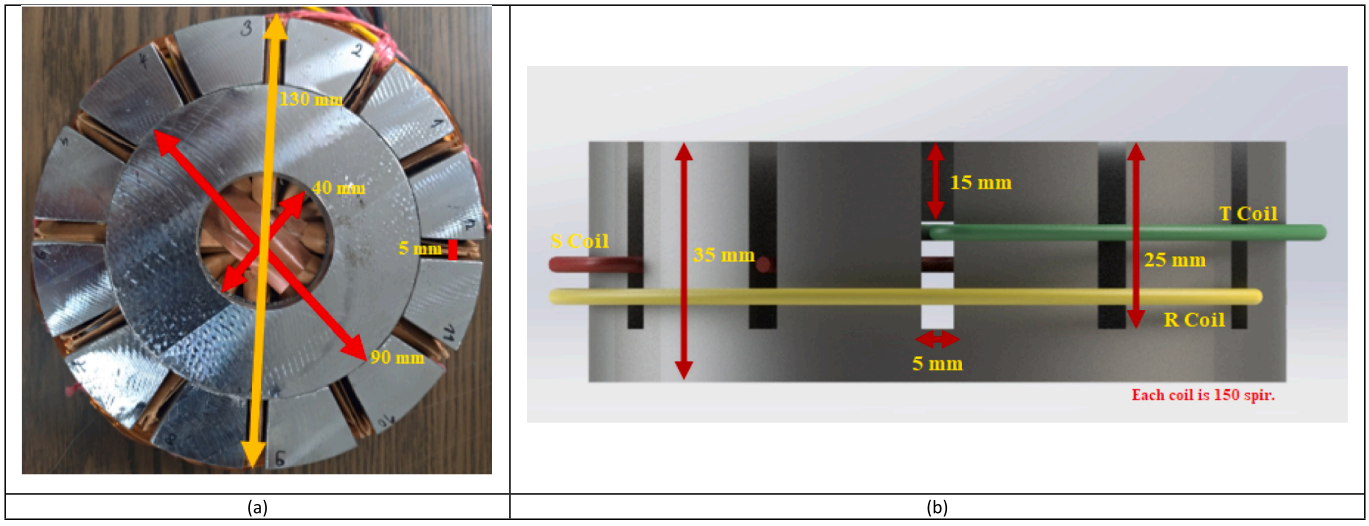

Fig. 8. Manufactured RMF Stirrer core (stator).

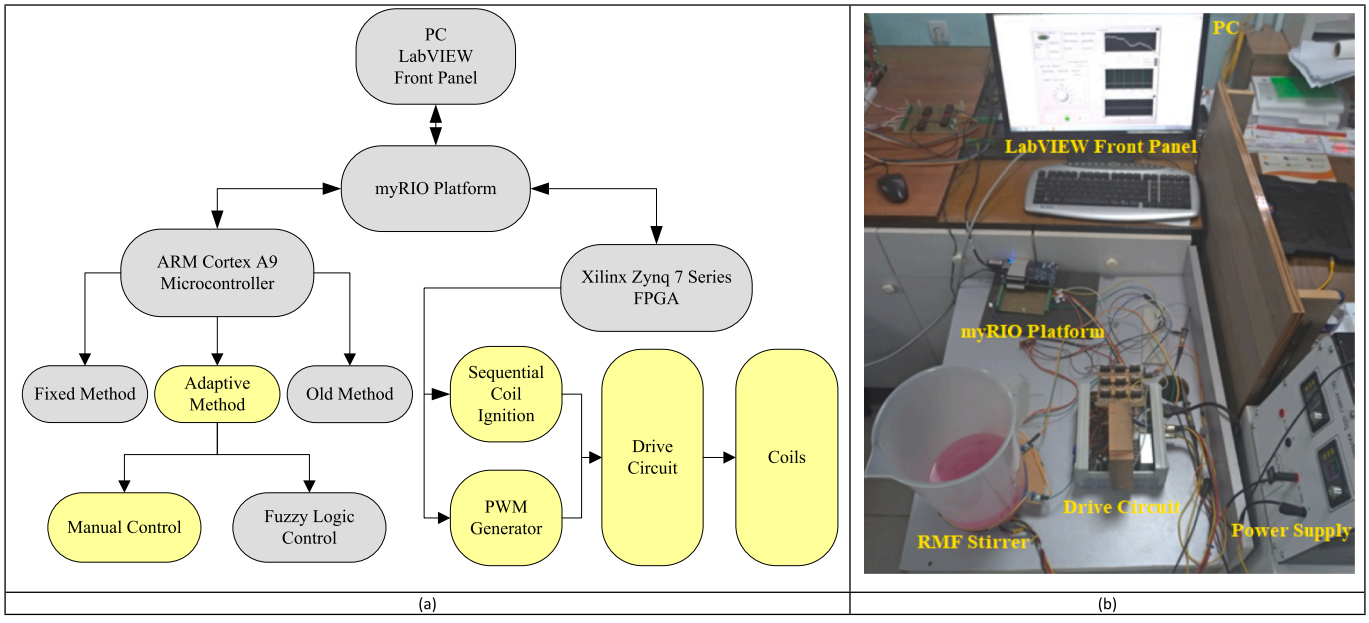

Fig. 9. A) block diagram, b) photograph of the developed rmf stirrer system.

system are energized under the control of myRIO® platform as shown in Fig. 9a. Microprocessor and FPGA modules of myRIO® were used in cooperation for energizing the coils. The basic control software that fires the coils to create the rotating magnetic field is run on the FPGA module on myRIO® (National Instruments Corporation, Austin, TX ABD). There are 2 algorithms running in parallel on the FPGA module. The first one is the algorithm that fires the coils in the appropriate sequence and timing according to the setting parameters from the microprocessor (Fig. 10) and the second one is the algorithm that generates the PWM signal according to the frequency and duty value from the microprocessor (Fig. 11). The pseudo-code for the FPGA algorithms is given in Appendix C. The algorithm that fires the coils provides the firing of the 3 coils

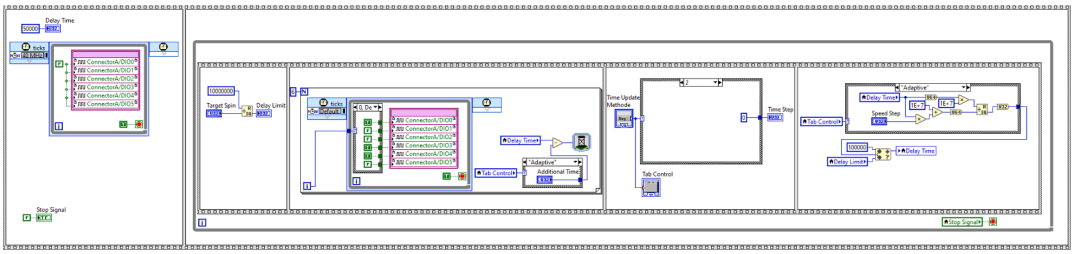

Fig. 10. LabVIEW® block diagram of sequential coil ignition circuit.

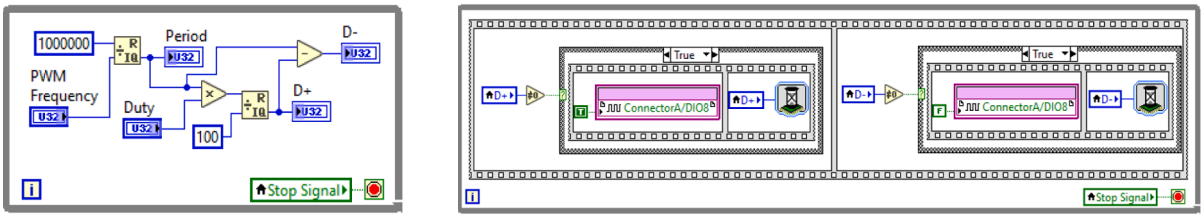

Fig. 11. LabVIEW® block diagram of PWM generator circuits: (a) timing calculator circuit, (b) PWM output control circuit.

shown in Fig. 2a according to the current inputs in the RST phases. In the algorithm, the waiting times required for the initial speed value of 100 rpm, which is the initial speed value at which the fish starts to rotate, are used for the firing timing of the coils. The waiting times required for the following firing timings are determined in the algorithm with Adaptive, Fixed, and Old methods according to the control input from the microprocessor. In the Adaptive method, the next waiting times are calculated according to the current speed of the magnetic fish, in the Fixed method, the waiting times are increased and decreased in fixed steps until the target speed value is reached, and in the Old method, the waiting times are decreased in incremental steps until the target speed value is reached. The obtained coil firing signals (Algorithm 1) and PWM signal (Algorithm 2) are transferred from the digital pins of myRIO® and applied to the coils through the driver circuit as shown in Fig. 9a.

The microprocessor module of myRIO® contains a control algorithm that determines the setting parameters of the 2 algorithms in the FPGA (Fig. 12). In this control algorithm, there is a reference speed generation sub-loop that generates the target speed value desired for the magnetic fish to rotate as a periodic wave or constant value. For the periodic reference speed, the frequency and speed variation value is entered by the user and a square wave signal with a center value of 300 rpm is obtained from the reference speed generator. The constant reference speed is taken as the value entered by the user. However, in the control algorithm in the microprocessor, the coil currents are read from the sensor and filtered with the moving window filter, the coil firing method for the FPGA is selected by the user and the frequency value required for the PWM and its duty value are determined. The duty value can be set by Fuzzy Logic or manually according to the user's choice (Fig. 13).

In the study, the adaptive control method was chosen for the coil firing method and the manual control method was chosen for the duty cycle value of the PWM signal. The manual controller operates at the loop time (10 ms) entered from the LabVIEW® interface and sends commands such as reference value, PWM frequency, N filter as input to the algorithms in the FPGA. In the interface, the reference value is the target speed of the magnetic fish, the PWM frequency is the frequency of the PWM signal, and the N filter is the number of elements of the moving window filter used to eliminate noise components in the measurement of coil currents. In this study, the reference value was chosen as 400 rpm, the PWM frequency as 10 kHz, and the N filter as 200 elements. The manual control duty cycle value can be changed manually in the range of 0–100 using the adjustment knob. However, in this study, this value is set to 100 %. In addition, the duty cycle value can also be adjusted by the fuzzy logic control method. By reducing the duty cycle value of the PWM signal with fuzzy logic control, the average voltage applied to the coils is reduced without affecting the rotation speed of the magnetic fish, and energy saving can be obtained. However, when the duty cycle value of the PWM signal decreases below 100 %, it is determined that the magnetic fish cannot rotate at 400 rpm, so the Manual control method is preferred instead of Fuzzy logic control. In addition, the aim of the study is not to increase the energy efficiency of the system.

6. Experimental finding

A series of experiments were conducted, which exhibited that the new magnetic stirrer developed within the scope of the study performed the stirring process both more homogeneously and within a shorter period of time. A second magnetic stirrer was utilized in such context, which was made of the same material bud could only rotate a single magnetic fish at the center (Fig. 14) [26]. Both stirrers were driven at 100 % duty cycle using Manual control and a rotating magnetic field was created by applying 24 W (16 V, 1.5 A) to the RST coils of the stirrers. Water was chosen as the liquid, in order to more easily observe the stirring process of the stirrers. One and four magnetic fish were respectively placed into two beakers, each containing 1 L of water, and the beakers were positioned on the stirrer cores. 2 ml of diluted red acrylic paint was added into the water in the beakers while the magnetic fish were rotating at 50 rpm, and the times elapsed for homogeneous distribution of the paint in the water were measured by taking video recordings (30 fps) (Fig. 15). The same processes were repeated by increasing the speed of the magnetic fish by 50 rpm up to 400 rpm. The time needed to obtain a homogeneous mixture was found to be 34 % shorter with the new stirrer. It has been determined that the time to reach homogeneity for different speeds is repeatable using the visual method. In addition, the vortex caused by a single magnetic fish rotating in the center was not seen in the newly-designed stirrer, due to multiple magnetic fish rotating in opposite directions. Thus, a mixture similar to that in an MHD stirrer was obtained without the need for a TMF stirrer. In the study, the experiments were repeated by changing the rotation

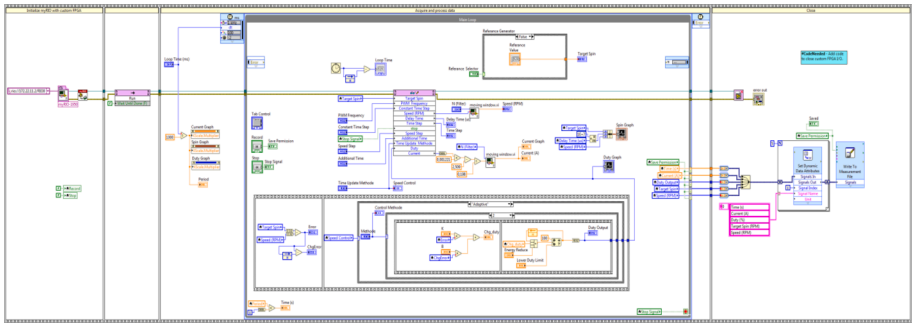

Fig. 12. LabVIEW® block diagram of microprocessor program.

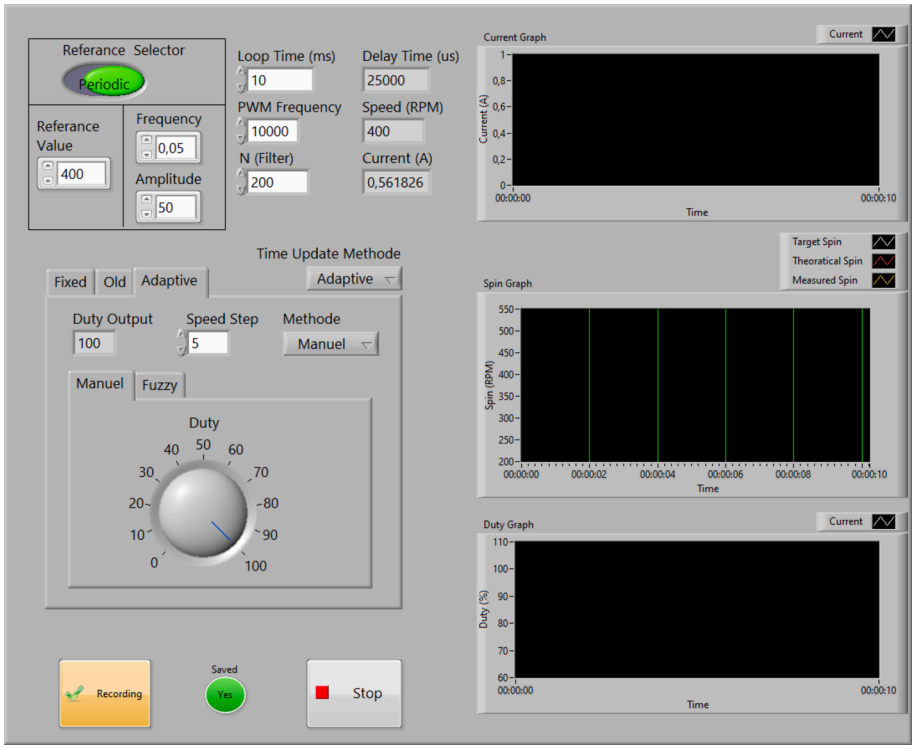

Fig. 13. LabVIEW® Front Panel of microprocessor program.

Fig. 14. A) magnetic stirrer which can rotate a single magnetic fish at the center, b) new magnetic stirrer which can rotate four magnetic fish.

speed up to 400 rpm with 50 rpm intervals, and the results are given in Table 2. It was additionally observed that the magnetic fish in the new stirrer drifted due to centrifugal force and rotation ended at speeds over 410 rpm. However, it is possible to increase the rotation speed of the magnetic fish above this value by increasing the magnitude of the magnetic field provided by the stirrer core. In order to increase the magnitude of the magnetic field provided by the stirrer core, it can be done by increasing the power values supplied to the system (24 W).

7. Conclusion and recommendation

This study aimed to develop a novel FPGA-based RMF stirrer system in order to reduce mixing time. A new RMF stirrer design was created within such scope, based on the results of magnetic analyses conducted using ANSYS Maxwell® simulation software, incorporating four magnetic fish rotating at symmetrical positions. The new stirrer was manufactured in the exact specifications shown in the design, and experiments conducted at various rotation speeds indicated that the new stirrer obtained a homogeneous mixture in a shorter period of time, compared to a second magnetic stirrer incorporating a single rotating magnetic fish at the center. Findings evidenced that the new stirrer reduced the time needed for a homogeneous mixture by 35 % in average, and eliminated the creation of a vortex in the stirring process. Thus, using said newly-designed RMF stirrer, a mixture similar to that in an MHD stirrer was obtained without the need for a TMF stirrer. In addition, it was observed that the magnetic fish in the new stirrer drifted due

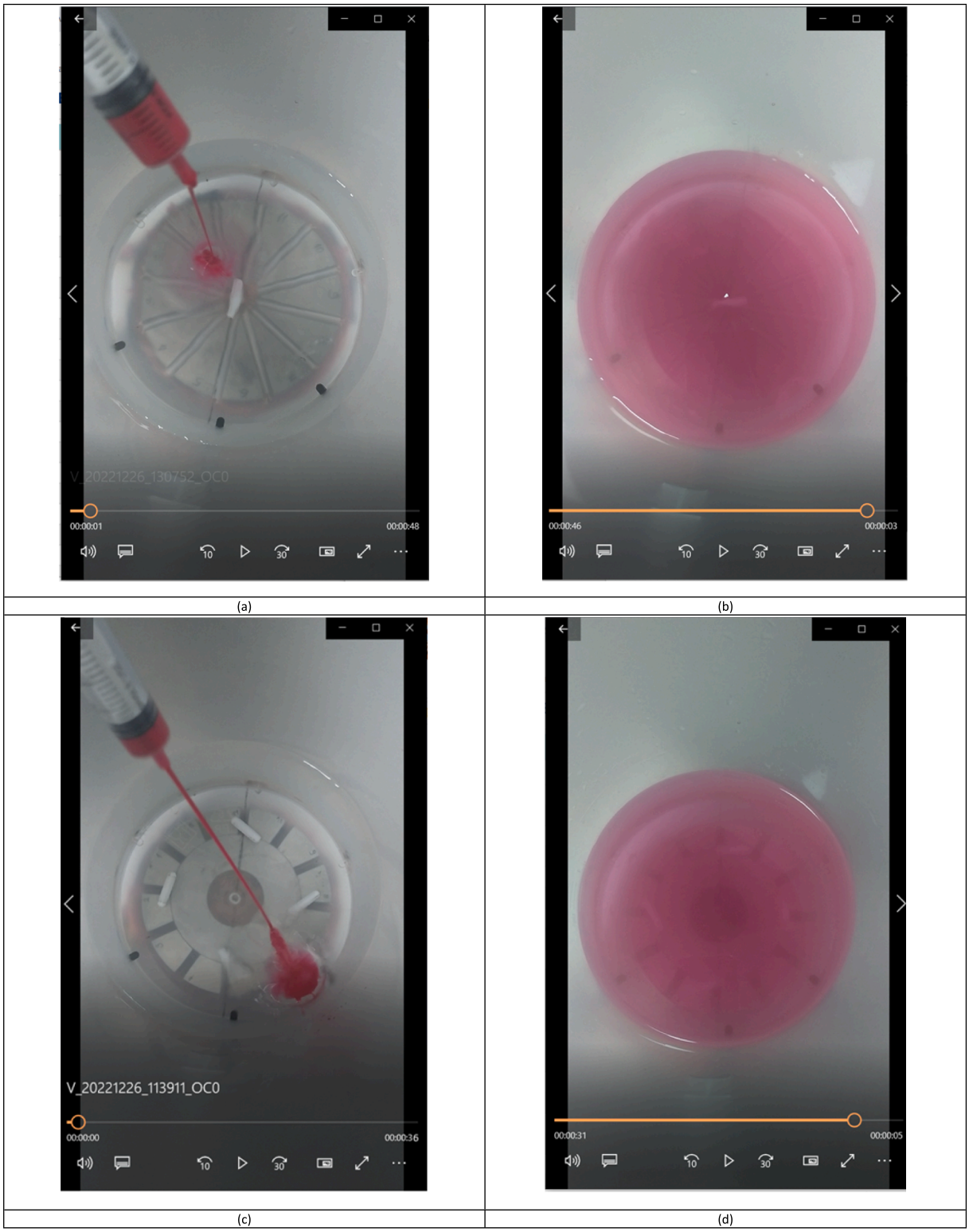

Fig. 15. Determination of homogeneous mixture time in a, b) Magnetic Stirrer inducing rotation at the center, and c, d) Newly-designed Magnetic Stirrer.

to centrifugal force and rotation ended at speeds over 410 rpm. However, it would be possible to increase the rotation speed of the magnetic fish above 410 rpm without drifting, by increasing the magnitude of the magnetic field created by the stirrer core. This may be achieved by increasing the current applied to the RST coils, using a stirrer core with greater magnetic permeability or increasing the number of windings.

Further, the duty cycle value for the PWM signal driving the stirrer via Adaptive control method in the LabVIEW® software developed for the new stirrer can be adjusted both manual and via fuzzy logic control. It is proposed that running the system with duty cycle values less than 100 % would improve energy efficiency. However, continuous rotation of the magnetic fish could not be achieved in the new stirrer under duty cycle values less than 100 %. This may be due to the decrease in current as a result of decreased duty cycle and the resulting decrease in magnetic

Table 2
Homogeneous mixture times of the stirrers by rotation speed.

Rotation Speed (rpm)	Homogeneous mixture time for the Magnetic Stirrer inducing rotation at the center (s)	Homogeneous mixture time for the newly-designed Magnetic Stirrer (s)	Percentage Difference (%)
50	46	30	34
100	40	25	38
150	35	23	36
200	30	21	30
250	26	16	38
300	21	13	39
350	19	13	30
400	16	10	33

force, which caused failure in synchronization of the rotation speed of the magnetic fish with the speed of phase change. However, the magnitude of the rotating magnetic field applied to magnetic fish can be increased by increasing the power consumption of the RMF stirrer above 24 W. Then, the minimum possible value of the increased power consumption can be determined manually or using a fuzzy logic controller.

CRediT authorship contribution statement

S. Bicakci: Writing – review & editing, Software, Methodology. **H. Citak:** Writing – review & editing, Methodology. **H. Gunes:** Writing – review & editing, Software. **M. Coramik:** Writing – review & editing, Methodology, Investigation. **Y. Ege:** Writing – review & editing, Writing – original draft, Software, Methodology, Investigation.

Appendix A

The change in magnetic field magnitude along 3 polylines for the S phase and T phase at the first position where the magnetic fish can rotate is given in Fig.A1. The magnetic field change graphs determined for R phase at the same position are given in Fig. 4.

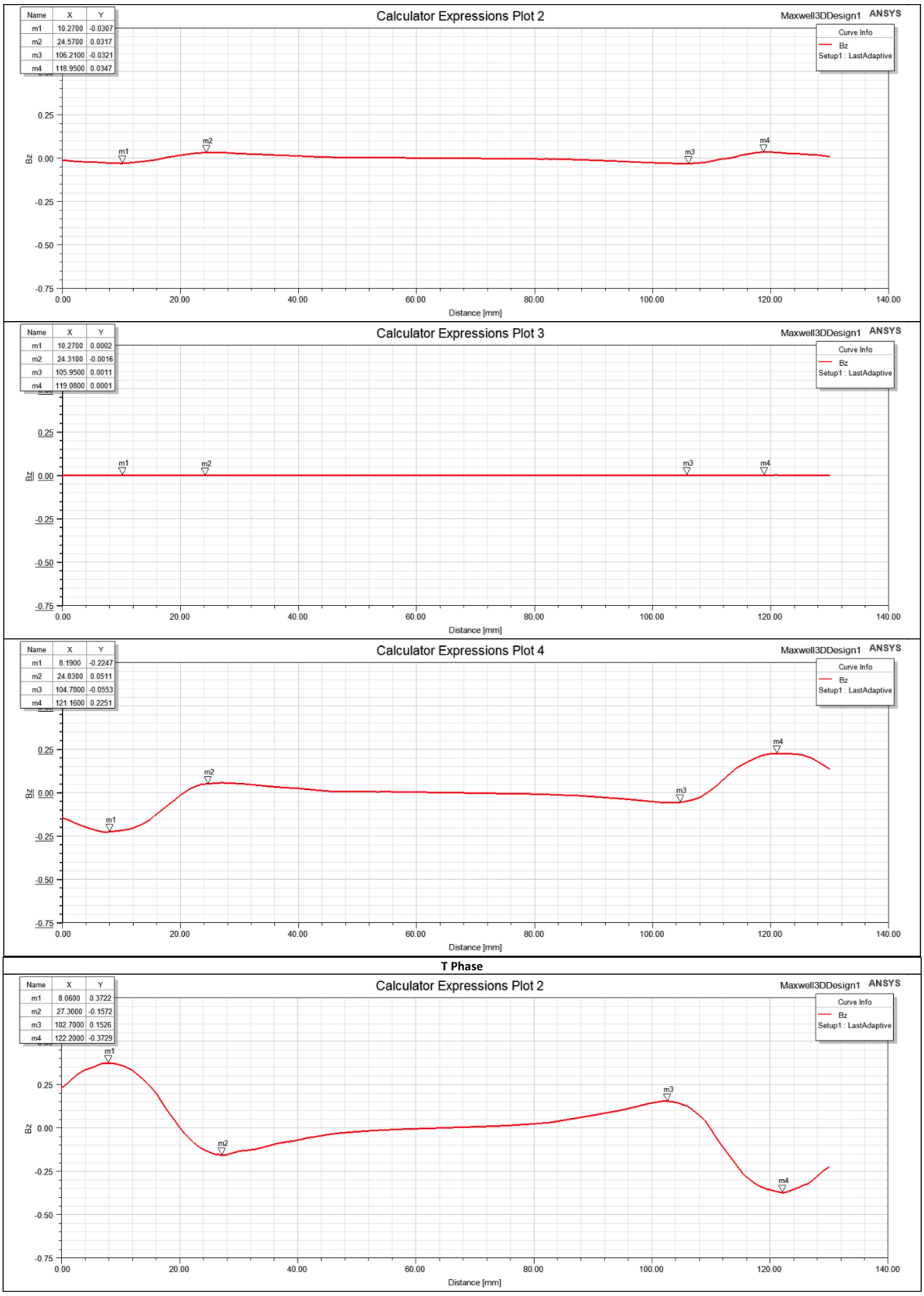

Fig. A1. Change in magnetic field magnitude along 3 polylines at the first position where the magnetic fish can rotate on the surface of the Magnetic Stirrer core (for S Phase and T Phase respectively)

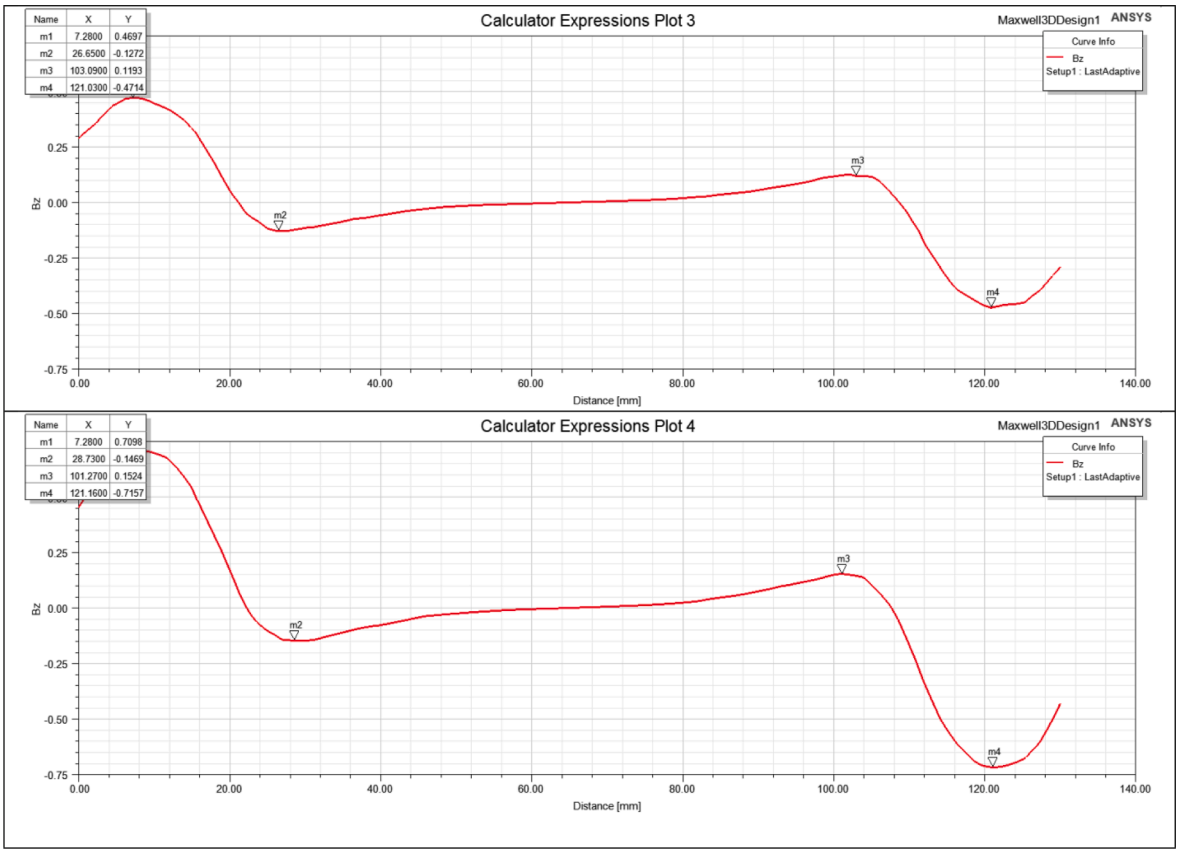

Fig. A1. (*continued*).

Appendix B

The change in magnetic field magnitude along 3 polylines for the R phase, S phase and T phase at the second position where the magnetic fish can rotate is given in Fig.B.1.

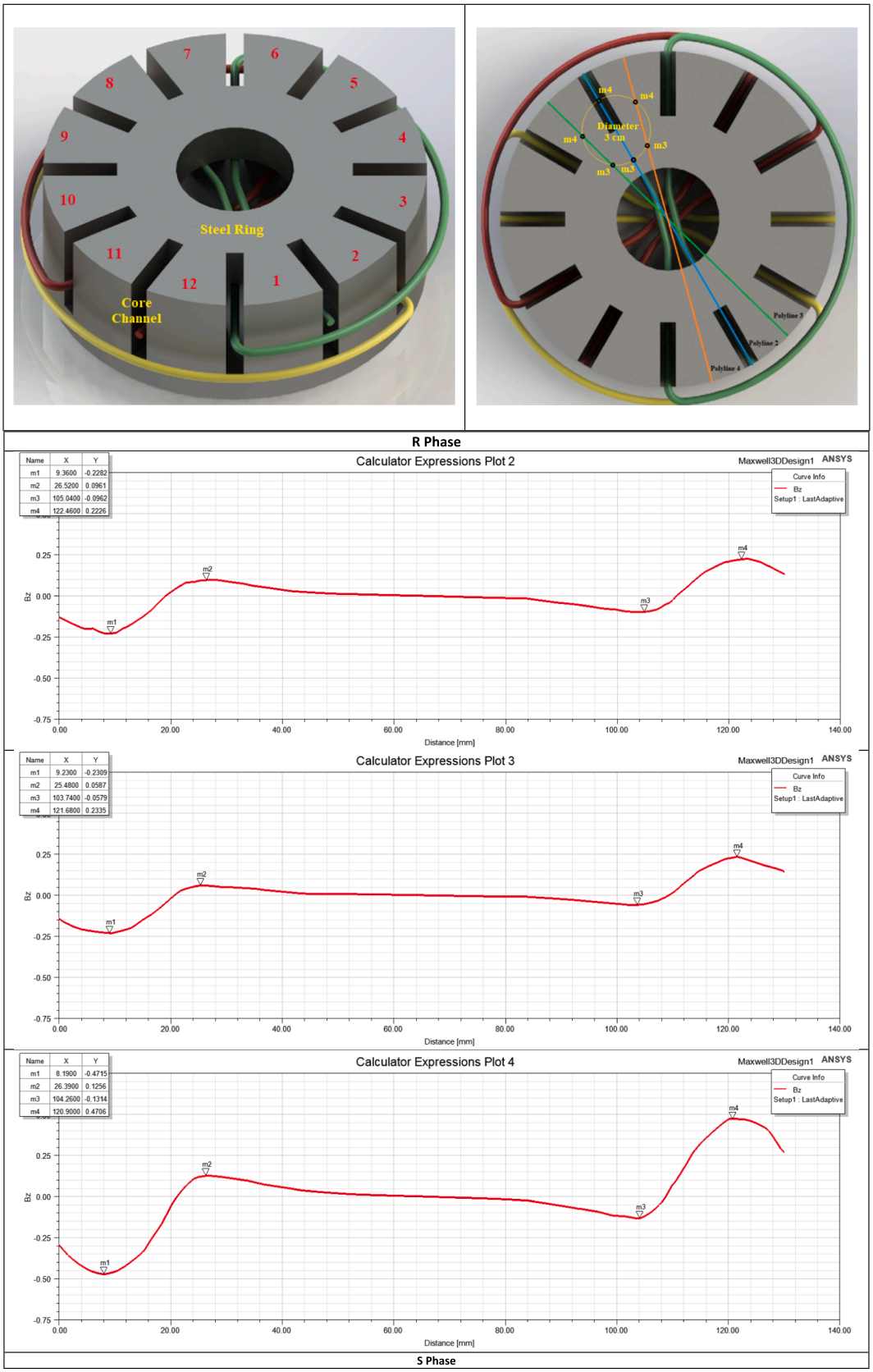

Fig. B1. Change in magnetic field magnitude along 3 polylines at the second position where the magnetic fish can rotate on the surface of the Magnetic Stirrer core (for R Phase, S Phase and T Phase respectively)

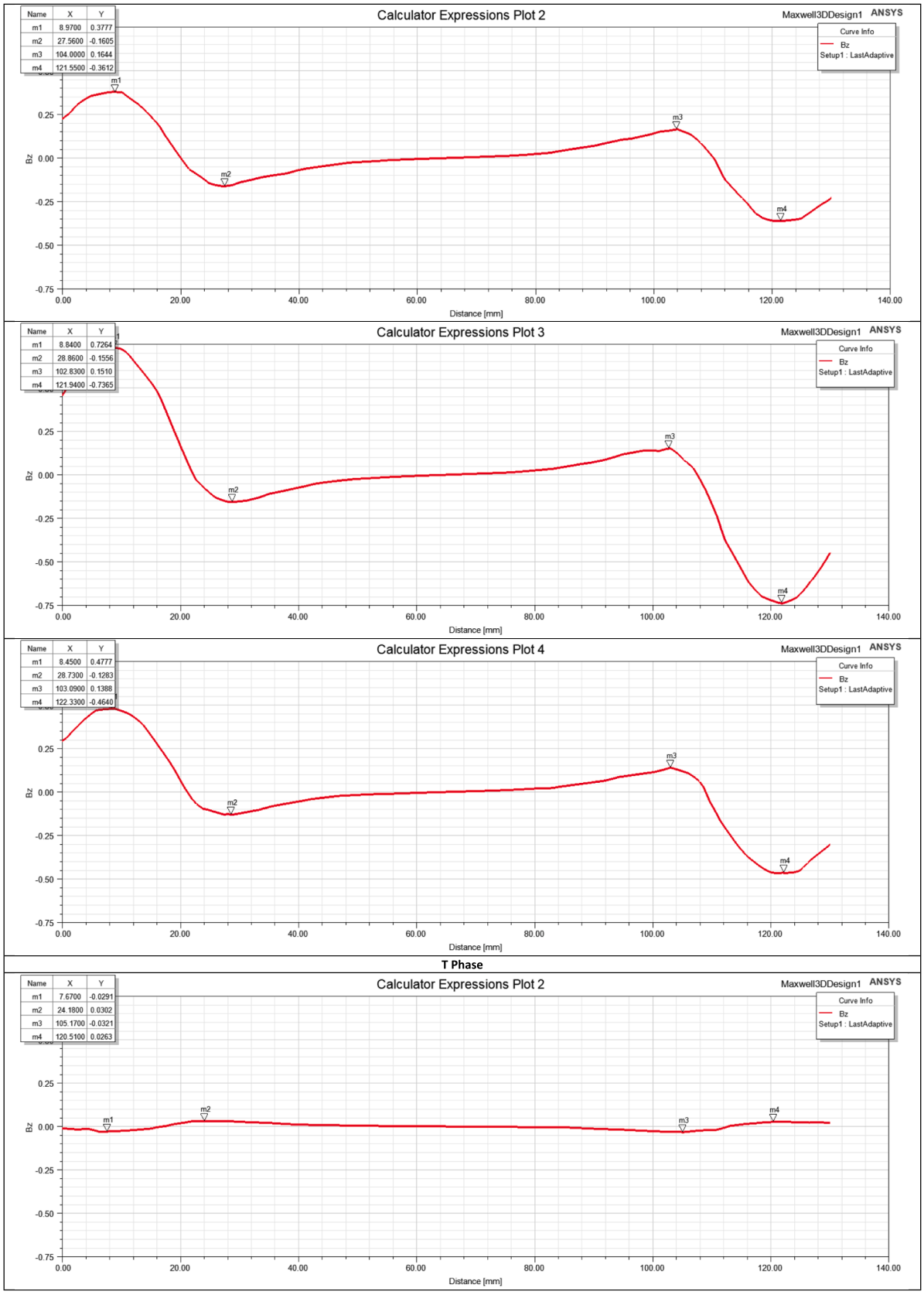

Fig. B1. (*continued*).

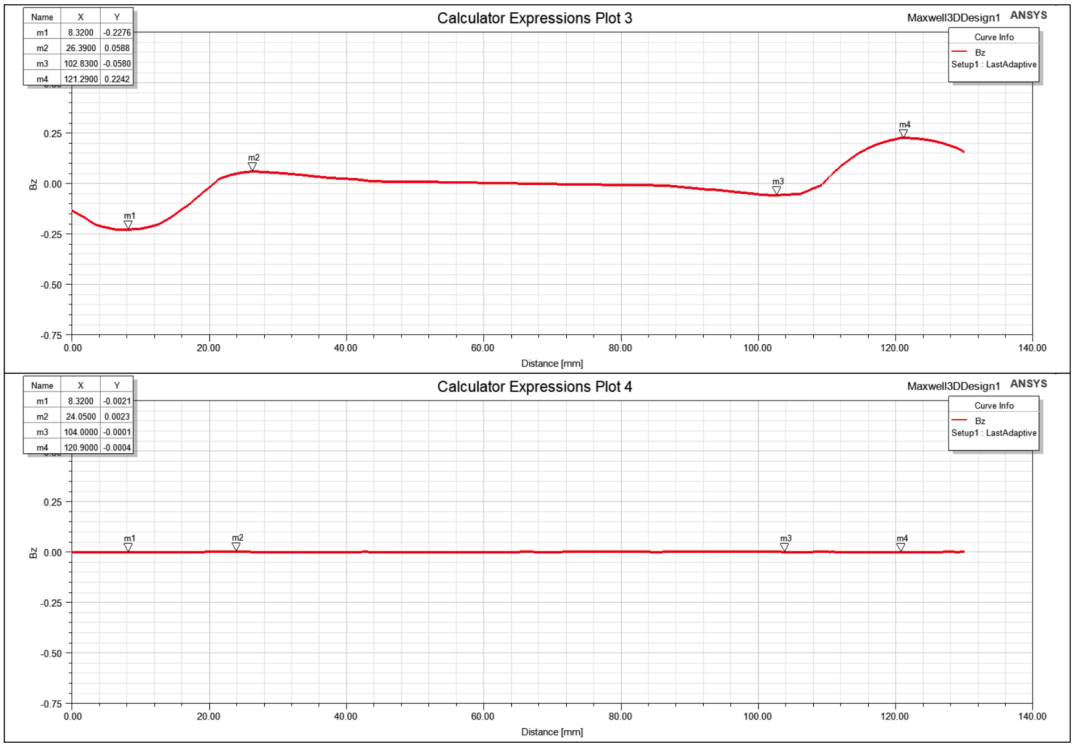

Fig. B1. (*continued*).

Appendix C

.

FPGA Parallel Algorithm – 1

Start
Initialize coil outputs
Set initial transition time (according to 100 RPM) –> **coil_transition_time**
Repeat:
Read target speed value –> **target_speed** (from Microprocessor program)
Fire coils sequentially with the determined transition time <- **coil_transition_time**
Read Control Method (Adaptive, Fixed, Old) –> **control_method** (from Microprocessor program)
Calculate fish turning speed value –> **fish_turning_speed**
If fish_turning_speed!= **target_speed** (400 RPM)
Switch(control_method):
Case Adaptive:
Calculate new coil transition time based on fish speed –> **coil_transition_time**
Case Fixed:
Calculate coil transition time with fixed steps –> **coil_transition_time**
Case Old:
Calculate coil transition time with stepped increments –> **coil_transition_time**

FPGA Parallel Algorithm – 2 –> PWM Generation Algorithm

Start
Repeat:
Read desired PWM frequency –> **pwm_frequency** (from Microprocessor program)
Read duty cycle value –> **duty** (from Microprocessor program)
Generate PWM signal

Microprocessor Algorithm

Start
Repeat:
Prompt user input –> **pwm_frequency**
Send to FPGA –> **pwm_frequency**
Prompt user input –> **target_fish_speed**
Prompt user input –> **reference_selector** (Periodic, Fixed)

(*continued on next page*)

(*continued*)

Microprocessor Algorithm
Switch(reference_selector):
Case Periodic:
Prompt user input −> **speed_change_value**
Prompt user input −> **periodic_signal_frequency**
Calculate periodic target speed signal −> **target_speed**
Case Fixed:
Prompt user input −> **target_speed**
Send to FPGA −> **target_speed**
Read coil current value −> **coil_current**
Prompt user input −> **filter_window_value** (200)
Calculate filtered current value (Moving Window Average)
Prompt user input −> **control_method**
Send to FPGA −> **control_method**
Prompt user input −> **duty_method**
Switch(duty_method):
Case Fuzzy:
Prompt user input −> **fuzzy_setting_values**
Determine new duty cycle value −> **duty**
Case Manual:
Prompt user input −> **duty**
Send to FPGA −> **duty**
Read from FPGA −> **fish_turning_speed**

References

[1] S.I. Shakhov, et al., Magnetohydrodynamic Simulation in the Progress of Electromagnetic Stirrers Designing. Part 2. Simulation of Magnetohydrodynamic Processes, Metallurgist 66(5–6) (2022) 639–645, https://doi.org/10.1007/s11015-022-01370-7.

[2] E.L. Shvydkii, et al., Impurity Distribution in a Two-Sided Electromagnetic Stirrer, Russian Metallurgy (metally) 2019 (6) (2019) 570–575, https://doi.org/10.1134/S0036029519060156.

[3] H. Jeon, M. Mehrdad, K. Jeongho, Magneto-hydrodynamics-driven mixing of a reagent and a phosphate-buffered solution: A computational study, Applied Mathematics and Computation 298 (2017) 261–271, https://doi.org/10.1016/j.amc.2016.11.026.

[4] A. Affanni, G. Chiorboli, Development of an enhanced MHD micromixer based on axial flow modulation, Sensors and Actuators b: Chemical 147 (2010) 748–754, https://doi.org/10.1016/j.snb.2010.03.077.

[5] A. Dehghan, et al., Integrated microfluidic system for efficient DNA extraction using on-disk magnetic stirrer micromixer, Sensors and Actuators b: Chemical 351 (2022) 130919, https://doi.org/10.1016/j.snb.2021.130919.

[6] S.H. Park, et al., Deep Transfer Learning-Based Sizing Method of Permanent Magnet Synchronous Motors Considering Axial Leakage Flux, IEEE Transactions on Magnetics 58 (9) (2022) 8206005, https://doi.org/10.1109/TMAG.2022.3181804.

[7] M. Horiuchi, et al., Effect of Magnetic Wedge Characteristics on Torque Ripple and Loss in Interior Permanent Magnet Synchronous Motor, IEEJ Journal of Industry Applications 11 (1) (2022) 49–58, https://doi.org/10.1541/ieejjia.21002574.

[8] Y. Ege, O. Kalender, S. Nazlibilek, Electromagnetic stirrer operating in double axis, IEEE Transactions on Industrial Electronics 57 (7) (2009) 2444–2453, https://doi.org/10.1109/TIE.2009.2034676.

[9] O. Kalender, Y. Ege, A PIC microcontroller based electromagnetic stirrer, IEEE Transactions on Magnetics 43 (9) (2007) 3579–3585, https://doi.org/10.1109/TMAG.2007.902825.

[10] M.M. Aboutalebi, et al., Numerical modelling of fluid flows in square billet moulds, using a new nozzle orientation in the presence of an in-mould rotary electromagnetic stirrer, Ironmaking & Steelmaking 46 (9) (2019) 819–826, https://doi.org/10.1080/03019233.2018.1510874.

[11] A. Ya Simonovsky, et al., Waves Formation in Capillary Volumes of Magnetic Fluid, Applied Engineering Letters 7 (3) (2022) 118–124, https://doi.org/10.18485/aeletters.2022.7.3.4.

[12] T.H. Naghash, et al., Performance of microball micromixers using a programmable magnetic system by applying novel movement patterns, Sensors and Actuators b: Chemical 406 (2024) 135403, https://doi.org/10.1016/j.snb.2024.135403.

[13] P.A. Nikrityuk, K. Eckert, R. Grundmann, Contactless Mixing of Liquid Metals, Metal Mater Trans B 41 (2010) 94–111, https://doi.org/10.1007/s11663-009-9320-5.

[14] B. Mikhailovich, O. Ben-David, A. Levy, Liquid metal rotating flow under permanent magnetic system impact, Magnetohydrodynamics 51 (1) (2015) 171–176, https://doi.org/10.22364/mhd.51.1.16.

[15] I. Kolesnichenko, et al., The study of turbulence in MHD flow generated by rotating and traveling magnetic fields, Experiments in Fluids 56 (88) (2015) 1–11, https://doi.org/10.1007/s00348-015-1957-z.

[16] M. Itamura, et al., Development of Generation Technology of High Quality Semi-Solid Slurry by Double-Axis-Electromagnetic Stirrer combined with Properly Designed Cup, Solid State Phenomena 192 (2013) 441–446, https://doi.org/10.4028/www.scientific.net/SSP.192-193.441.

[17] S. Taniguchi, et al., Electromagnetic stirring of liquid metal by simultaneous imposition of rotating and traveling magnetic fields, Tetsu-to-Hagané 92 (6) (2006) 364–371, https://doi.org/10.2355/tetsutohagane1955.92.6_364.

[18] K. Bolotin, et al., Shape optimization of soft magnetic composite inserts for electromagnetic stirrer with traveling magnetic field, COMPEL-the International Journal for Computation and Mathematics in Electrical and Electronic Engineering 39 (1) (2020) 28–35, https://doi.org/10.1108/COMPEL-05-2019-0207.

[19] V.K. Gupta, K.J. Pradeep, K.J. Pramod, A novel approach to predict the inclusion removal in a billet caster mold with the use of electromagnetic stirrer, Journal of Manufacturing Processes 83 (2022) 27–39, https://doi.org/10.1016/j.jmapro.2022.08.048.

[20] K. Bolotin, et al., Numerical simulation of the electromagnetic stirrer adapted by using magnetodielectric composite, Magnetohydrodynamics 53 (4) (2017) 723–730, https://doi.org/10.22364/mhd.53.4.14.

[21] S. Khripchenko, et al., Use of a travelling magnetic field“ ROD” inductor for stirring molten metal in an aluminum bath, Magnetohydrodynamics 52 (3) (2016) 407–416, https://doi.org/10.22364/mhd.52.3.8.

[22] N. Dropka, F.R. Christiane, P. Rudolph, Comparison of stirring efficiency of various non-steady magnetic fields during unidirectional solidification of large silicon melts, Journal of Crystal Growth 365 (2013) 64–72, https://doi.org/10.1016/j.jcrysgro.2012.12.009.

[23] M. Bayareh, M.N. Ashani, A. Usefian, Active and passive micromixers: A comprehensive review, Chemical Engineering and Processing-Process Intensification 147 (2020) 107771, https://doi.org/10.1016/j.cep.2019.107771.

[24] A. Cramer, et al., Electromagnetic stirring with superimposed travelling and rotating magnetic fields, Przegląd Elektrotechniczny 84 (11) (2008) 144–148, https://doi.org/10.12915/pe.2008.11.029.

[25] W. Bernd, et al., Experimental Investigations of Rotary Electromagnetic Mould Stirring in Continuous Casting Using a Cold Liquid Metal Model, ISIJ International 57 (3) (2017) 468–477, https://doi.org/10.2355/isijinternational.ISIJINT-2016-495.

[26] H. Citak, et al., A New RMF Stirrer Using AISI4140 Mild Steel: Energy Optimization Application, Electrical, Control and Communication Engineering 19 (1) (2023) 49–59, https://doi.org/10.2478/ecce-2023-0007.